

Coupling material and mechanical design processes via computer model calibration

Carl Ehrett*

School of Mathematical and Statistical Sciences, Clemson University,

D. Andrew Brown

School of Mathematical and Statistical Sciences, Clemson University,

Evan Chodora

Department of Mechanical Engineering, Clemson University,

Christopher Kitchens

Department of Chemical and Biomolecular Engineering, Clemson University,

and

Sez Atamturktur

Department of Architectural Engineering, Pennsylvania State University

October 18, 2019

Abstract

Computer model calibration typically operates by choosing parameter values in a computer model so that the model output faithfully predicts reality. By using performance targets in place of observed data, we show that calibration techniques can be repurposed to wed engineering and material design, two processes that are traditionally carried out separately. This allows materials to be designed with specific engineering targets in mind while quantifying the associated sources of uncertainty. We demonstrate our proposed approach by “calibrating” material design settings to performance targets for a wind turbine blade.

Keywords: Gaussian processes, material design, optimization, Pareto optimality, Uncertainty quantification, wind turbines

*The authors gratefully acknowledge *please remember to list all relevant funding sources in the unblinded version*

1 Introduction

Real-world optimization problems typically involve multiple objectives. This is particularly true in the design of engineering systems, where multiple performance outcomes are balanced against budgetary constraints. Among the complexities of optimizing over multiple objectives is the effect of uncertainties in the problem. Design is guided by models known to be imperfect, systems are built using materials with uncertainty regarding their properties, variations occur in the construction of designed systems, and so on. These imperfections, uncertainties and errors cause uncertainty also in the solution to a design problem.

In traditional engineering design, one designs a system after choosing a material with appropriate properties for the project from a database of known materials. As a result, the design of the system is constrained by the initial material selection. By coupling material discovery and engineering system design, we can combine these two traditionally separate processes under the umbrella of a unified multiple objective optimization problem.

In this paper, we cast the engineering design problem in the framework of computer model calibration. In traditional calibration, one aligns computer model output to observations of a real system by estimating unknown parameters in the model. Here, we instead align the computer model to performance and cost targets by finding design variables that optimize the model output with respect to those targets.

Our proposed methodology uses the Bayesian framework first established as a means for computer model calibration by Kennedy and O’Hagan (2001). This area is furthered by Higdon et al. (2004), who undertake model calibration with quantified uncertainty. The approach of Higdon et al. (2004) is further refined and exemplified by Williams et al.

(2006). Loepky et al. (2006) offer a maximum-likelihood-based alternative to the Bayesian approach advocated by Kennedy and O’Hagan, intending thereby to improve the identifiability of the calibration parameters in the face of model discrepancy. Bayarri et al. (2007) extend the approach of Kennedy and O’Hagan, allowing for simultaneous validation and calibration of a computer model. Bayarri et al. (2007) apply this methodology to functional data using a hierarchical framework for the coefficients of a wavelet representation. Similarly, Paulo et al. (2012) apply the approach of Bayarri et al. (2007) to computer models with multivariate output. Brynjarsdóttir and O’Hagan (2014) demonstrate the importance of strong priors on the model discrepancy term when undertaking calibration.

Common to those approaches is a conception of calibration as using real observations to get a posterior distribution on unknown parameters θ so that the posterior predictive distribution of the model approximates reality. By contrast, using an approach we call counterfactual Bayes, our methodology uses artificial observations (representing design targets) to obtain a posterior distribution on design variables θ so that the posterior predictive distribution approaches those targets. In counterfactual Bayes, we apply Bayesian reasoning to a hypothetical scenario that bears certain known relationships to reality. Those known relationships allow us to transfer knowledge gained about the hypothetical scenario to reality, thereby gaining valuable insights into the phenomenon of interest. We describe how, with little added computational cost, the methodology provides an initial rough estimate of the *Pareto front* for the system, i.e., the set of points in the design space that are Pareto optimal. A point is Pareto optimal if and only if, in order to improve any one of its elements, some other element must be made worse off. In a system in which there

is a trade-off between cost and performance, for example, which region of the Pareto front is most desirable will depend upon budgetary constraints. This initial rough estimate of the Pareto front can be used to select artificial observations closer to the design space and thereby promote stronger Bayesian learning about the optimal settings for the design variables θ . Repeated applications of the procedure can be used to produce the more thorough “Pareto bands” which estimate the Pareto front with quantified uncertainties.

Our approach is thus an example of Bayesian multi-objective optimization under uncertainty. Concerns about uncertainty in optimization may include uncertainty in the inputs (as when the inputs are not under perfect control), uncertainty in the outputs (as when the code or process of interest is not deterministic), and observation error (Jin and Branke, 2005). As a response to these sources of uncertainty, two different approaches are possible. Firstly, one’s focus may be on finding solutions that are robust to small perturbations in the inputs, e.g. by resampling in the design space around each candidate point considered during optimization (Deb and Gupta, 2006). Alternatively, rather than seeking robust solutions, one could endeavor simply to quantify the resulting uncertainty in the model outputs, again through resampling around points of interest (Zhou et al., 2011). Our focus is on the latter of these two goals, though the posterior distributions our method also provides include information about the sensitivity of the model output to the various model inputs, and thereby provides information about the robustness of the estimated optima. Since we are concerned with computationally expensive objective functions, our method also avoids resampling, which can add prodigiously to the computational expense of an optimization procedure.

Though a Bayesian means of optimization, our proposed methodology contrasts with what is typically referred to as “Bayesian optimization” (BO). In traditional BO, a Gaussian process (GP) surrogate model is constructed based on a small set of training observations, and the resulting updated GP is used to define an “acquisition function” that is used sequentially to select new observation locations until a stopping condition is achieved (Picheny et al., 2019). Acquisition functions are crafted to attempt to balance exploration with exploitation of the objective function. Examples include the EGO (efficient global optimization) function of Jones et al. (1998), and the EGO-inspired SUR (stepwise uncertainty reduction) function showcased for univariate BO by Chevalier et al. (2014). The SUR approach is applied to estimating the Pareto front of a multi-objective optimization problem by Picheny (2015). The methodology we propose here differs from these forms of traditional BO by its avoidance of sequential sampling, which is desirable in cases where the computational budget is very small, or when the relevant observations are based on previously gathered data, or in general when the data-gathering process is not devoted exclusively to serving the ends of the optimization. Our methodology also can be used to quantify all associated forms of uncertainty discussed above – uncertainty due to the model inputs, due to the stochastic nature of the objective function, or due to observation error of the outputs (e.g. if the observations are of the phenomenon of interest itself rather than of a computer model thereof).

Our approach thus has affinities with that of Olalotiti-Lawal and Datta-Gupta (2015). Both approaches use Markov chain Monte Carlo (MCMC; Gelfand and Smith, 1990) to explore a posterior distribution on the design inputs. Olalotiti-Lawal and Datta-Gupta

construct a distribution that is designed to lie both on and near the Pareto front of the objective function. The acceptance rate and the variance of the distribution depend upon a user-defined temperature parameter. The resulting posterior distribution includes uncertainty quantification. The uncertainty quantified here is the uncertainty remaining in the distribution designed by the authors, which is not itself part of the modeled phenomenon. By contrast, under our approach, the distribution explored via MCMC is dictated by the model itself (and by the GP surrogate thereof), and by the choice of performance/cost targets. The approach we propose here also has somewhat greater flexibility – while it may be used to explore the entire Pareto front as Olalotiti-Lawal and Datta-Gupta do, our approach also may be used as a form of “goal programming” (Miettinen, 2008), targeting a particular region of the Pareto front in accordance with the preferences of the relevant decision-makers.

We apply our proposed methodology both to a proof-of-concept example and to finding material design settings to optimize performance and cost for a wind turbine blade of fixed outer geometry. The blade is to be constructed using a composite material, the properties of which are dependent upon design variables under our control. Our material design goal is to reduce the cost per square meter of the composite, the angle of twist (in radians) of the blade when under load, and the deflection (in meters) of the blade tip when under load.

In Section 2, we introduce the counterfactual Bayes methodology we rely on for learning about a real system by applying Bayesian reasoning in a hypothetical scenario with known linkages to the real system. In Section 3, we review the calibration framework grounding our design optimization approach. In Sections 4 and 5, we apply our methodology to simulated

data and to wind turbine blade design. Section 6 discusses the results and thoughts about future directions.

2 Counterfactual Bayes

We introduce the approach used here using a simple thought experiment. Consider a golfing enthusiast, David, who has been challenged to hit a ball on a long narrow fairway as far as possible in a given direction from a given starting point on the fairway. David has at his disposal not merely the usual set of clubs; David is a collector with a dizzying array of woods appropriate to this challenge. They differ in loft angle (angle of the club head), in head material, in shaft material, in head volume, in shaft flexibility, shaft length, and so on. He knows that his drive distances are normally distributed with a common variance and a mean that varies based on the club, terrain and start point, but he does not know which club will produce the highest mean in this situation. However, David has a so-far untapped resource here. David has a savant-like ability, given an observation of a player, terrain, ball start point and end point, to guess the club used in that instance. Of course, David has not made any relevant observation in this case, but he realizes that he can apply his ability to a *hypothetical* observation of himself, the current terrain, his current start point and an end point of his choosing. He can reason as though he observed a particular extremely successful outcome, and thereby use his ability to identify which club would be most likely to have produced that outcome. Since his drive distances are normally distributed with common variance, he can infer that the club producing this extreme outcome is also the club having the optimal expected outcome in the hypothetical scenario. Finally, since the

model governing his drive distance is the same in the hypothetical scenario as in reality, he can conclude that the club he used in his hypothetical scenario is also the best choice for him to use in reality.

To generalize David’s reasoning, we rely on the logician’s conception of possible worlds, which are used to explain the semantics of modal sentences (sentences having to do with possibility and necessity, rather than what is merely actual). A possible world can be conceived of as an internally consistent description of a world, which may or may not match the actual world (Adams, 1974, though for an opposing perspective on modal ontology see Lewis, 1986). So even though it is perhaps true that all dogs weigh under 350lbs (the heaviest recorded dog weighed 343lbs; Young, 1994), there is a possible world in which some dogs weigh over 350lbs, since it is possible to describe such a world without contradicting oneself. I.e., a 350lb dog *could* exist. By contrast, there is no possible world in which some dogs are reptiles. Dogs are mammals by definition, and to describe any creature simultaneously as a reptile and as a dog is to contradict oneself. In the case of David, the fact that his drive distances follow a normal distribution allows us to infer there is a possible world in which he manages to hit a 300 yard fairway drive, without thereby contradicting our assumption that in this possible world his drive distances follow the same distribution they do in the actual world.

We can generalize the counterfactual methodology David employs as follows. Let α denote the actual world. Let f_α be a function relating inputs $\mathbf{x}, \boldsymbol{\theta}$ to some output \mathbf{y} , which describes some phenomenon of interest in the real world for which we wish to find optimal settings for $\boldsymbol{\theta}$. Suppose that f_α is such that the optimal outcome can be redescribed in

terms of some target outcome \mathbf{y}_t , i.e., that $\operatorname{argmin}_{\boldsymbol{\theta}} f_{\alpha}(\mathbf{x}, \boldsymbol{\theta}) = \operatorname{argmin}_{\boldsymbol{\theta}} \|\mathbf{y}_t - f_{\alpha}(\mathbf{x}, \boldsymbol{\theta})\|$. Then a distribution $\boldsymbol{\theta}|\mathbf{x}, \mathbf{y}_t$ *de facto* approximates a distribution on $\boldsymbol{\theta}$ values producing the optimal achievable output of the system. Consider now a possible world ω in which the same phenomenon $f_{\omega} = f_{\alpha}$ holds true, and in which we observe \mathbf{y}_t . Then we can apply Bayes' rule to learn a posterior distribution $p(\boldsymbol{\theta}|\mathbf{x}, \mathbf{y}_t)$ of $\boldsymbol{\theta}$ values in ω . This is not directly applicable to the actual world, since we have not observed \mathbf{y}_t here. But we have that $\boldsymbol{\theta}|\mathbf{x}, \mathbf{y}_t$ approximates a distribution on $\boldsymbol{\theta}$ values producing an optimal achievable outcome from the system f_{ω} , and we furthermore have that $f_{\alpha} = f_{\omega}$ and thus that a distribution on $\boldsymbol{\theta}$ values optimal for f_{ω} is also a distribution on $\boldsymbol{\theta}$ values optimal for f_{α} . Thus by relying on known connections between ω and α , we use observations made only in ω to gain valuable insight into features of α .

In what follows, we apply this counterfactual Bayes approach to find distributions on optimal design settings. In our approach, Kennedy-O'Hagan-style model calibration (Kennedy and O'Hagan, 2001) stands in for David's knack for identifying the "settings" (club choice) that produced a given observation. We will apply that model calibration framework in a hypothetical scenario involving artificial observations of idealized outcomes \mathbf{y}_t , using our knowledge of the true system to exploit the resulting posterior distribution $\boldsymbol{\theta}|\mathbf{y}_t$ and thereby discover a distribution on optimal design settings.

3 Calibration for design

3.1 Gaussian process emulators for calibration

In this work, when an emulator is needed we use GP emulators. As a multivariate Gaussian random variable is characterized by a mean vector and covariance matrix, a GP is characterized by a mean and covariance functions $\mu : D \rightarrow \mathbb{R}$ and $C : D \times D \rightarrow \mathbb{R}$, where D is the domain of the process. For points $\mathbf{x}, \mathbf{y} \in D$, $\mu(\mathbf{x})$ is the GP mean at \mathbf{x} , and $C(\mathbf{x}, \mathbf{y})$ is the covariance between the values of the GP at \mathbf{x} and \mathbf{y} . The distribution of the GP at any finite number of points is multivariate normal with mean vector and covariance matrix determined by $\mu(\cdot)$ and $C(\cdot, \cdot)$. In principle, model calibration need not rely on emulators; one can complete a Bayesian analysis via MCMC by running the model at each iteration of the chain (see e.g. Hemez and Atamturktur, 2011). In Section 4 we assume fast-running computer code for the simulated example, but computer models are often too computationally expensive to allow such expenditure (Van Buren et al., 2013, 2014). Instead, a computationally tractable emulator can be trained using a sample of the computer model output.

GPs are popular prior distributions on computer model output for three reasons. Firstly, their use does not require detailed foreknowledge of the model function’s parametric form. Secondly, GPs easily interpolate the computer model output, which is attractive when the model is deterministic and hence free of measurement error. This is the usual case, although some attention (e.g., Pratola and Chkrebtii, 2018) has focused on calibrating stochastic computer models. Thirdly, GPs facilitate uncertainty quantification through the

variance of the posterior GP. This section provides brief background on GPs and their use in regression broadly, and in computer model calibration specifically.

The use of GPs as a computationally efficient predictor of computer code given observations of code output is advocated by Sacks et al. (1989) and explored at length by Santner et al. (2003). Since computer code is typically deterministic, these applications differ from the focus of O’Hagan (1978) in that the updated GP interpolates the computer output. Kennedy and O’Hagan (2001) use GPs for computer model calibration. Kennedy et al. (2006) showcase this use of GP emulators for uncertainty and sensitivity analyses. Bastos and O’Hagan (2009) describe numerical and graphical diagnostic techniques for assessing when a GP emulator is successful, as well as likely causes of poor diagnostic results. Though most work on GP emulation uses stationary covariance functions and quantitative inputs, Gramacy and Lee (2008) use treed partitioning for a nonstationary computer model, and Qian et al. (2008) explore methods that include both quantitative and qualitative inputs.

Whether or not an emulator is used, one may consider a computer model to be of the form $\eta(\mathbf{x}, \boldsymbol{\theta})$, where $(\mathbf{x}, \boldsymbol{\theta})$ comprise all model inputs. The vectors $\boldsymbol{\theta}$ and \mathbf{x} denote respectively the inputs to be calibrated and the *control inputs*, which are all other model inputs that are known and/or under the researchers’ control. Thus, the model is

$$y(\mathbf{x}) = \eta(\mathbf{x}, \boldsymbol{\theta}) + \delta(\mathbf{x}) + \epsilon(\mathbf{x}), \quad (1)$$

where $y(\mathbf{x})$ is the response at control inputs \mathbf{x} , $\delta(\cdot)$ is the model discrepancy (the systematic bias of the model) and $\epsilon(\cdot)$ is mean-zero error, often assumed to be i.i.d. Gaussian.

To use an emulator, suppose we have inputs $\{(\mathbf{x}_i, \mathbf{t}_i)\}_{i=1}^n \subseteq \mathbb{R}^p \times \mathbb{R}^q$ scaled to the unit hypercube and completed model runs $\eta(\mathbf{x}_i, \mathbf{t}_i)$ for $i = 1, \dots, n$. Define the GP prior for

$\eta(\cdot, \cdot)$ as having mean function $\mu(\mathbf{x}, \mathbf{t}) = c$, where c is a constant, and set the covariance function in terms of the marginal precision λ_η and a product power exponential correlation:

$$C((\mathbf{x}, \mathbf{t}), (\mathbf{x}', \mathbf{t}')) = \frac{1}{\lambda_\eta} \prod_{k=1}^p \exp(-\beta_k^\eta |x_k - x'_k|^{\alpha_\eta}) \times \prod_{j=1}^q \exp(-\beta_{p+j}^\eta |t_j - t'_j|^{\alpha_\eta}) \quad (2)$$

where each β_k describes the strength of the GP's dependence on one of the elements of the input vectors \mathbf{x} and \mathbf{t} , and α_η determines the smoothness of the GP. The model is completed by specifying priors for the hyperparameters c , λ_η , α_η , and β_j^η for $j = 1, \dots, p + q$, though in practice these are often set to predetermined values.

3.2 Design to target outcomes

Call design targets treated as observations in the design procedure we propose below “target outcomes”, and call that procedure, which pairs a Bayesian model calibration framework with target outcomes via counterfactual Bayes, “calibration to target outcomes” (CTO). Thus target outcomes are a sort of artificial data, and the calibration procedure is carried out as if these artificial data had been observed in reality. As in traditional calibration, in which the result is a distribution on the calibrated parameter $\boldsymbol{\theta}$ to approximate the observed data, in CTO the result is a distribution on the design parameter $\boldsymbol{\theta}$ which induces the model to approximate the performance and cost targets.

The tools of model calibration as based on the work of Kennedy and O'Hagan (2001) retain their advantages under our proposed methodology. Most centrally, calibrating to target outcomes \mathbf{y} produces not merely a point estimate \mathbf{t}^* , but rather a posterior distribution of $\mathbf{t}|\mathbf{y}$ reflective of remaining uncertainty about the optimal value of \mathbf{t}^* . Such uncertainty may come from parameter uncertainty (uncertainty about the values of model inputs other

than the design variables), model form uncertainty (uncertainty about how closely the code approximates reality), and observation error. The Bayesian model calibration framework allows for quantification of all of these uncertainties.

If a model discrepancy term $\delta()$ is included as in Equation (1), an informative prior must be used to mitigate the identifiability concerns of the Kennedy-O’Hagan (Bayarri et al., 2007; Tuo and Wu, 2016). Otherwise, the estimate of the design variables may be compromised by the flexibility of the discrepancy function. That is, with a flexible $\delta()$ which is not constrained to approximate a true discrepancy between the model $\eta()$ and reality $y()$, the distance from the feasible objective space to the target outcomes may be “absorbed” by $\delta()$, rather than being minimized by finding the optimal value of $\boldsymbol{\theta}$. Essentially, in such a case, the algorithm would use $\delta()$ to *move* the feasible design space to the target outcomes, rather than finding the point in the true feasible design space that is closest to the targets. To prevent this, the model $\eta()$ should be calibrated well enough that the discrepancy $\delta()$ between its output and reality is known to be small (or zero), so that an informative (or degenerate) prior can be placed on $\delta()$ during CTO ensuring that the posterior discrepancy remains small (or zero).

Target outcomes should aim only a little beyond the feasible region; only as far as required to ensure the targets are at least as ambitious as any feasible optimum. This is because, firstly, target outcomes that are too farfetched may cause the procedure to be computationally unstable due to underflow and round-off error, since any value of $\boldsymbol{\theta}$ within its support will have extremely low likelihood. Secondly, increasing the distance of the target outcomes from the optimal region reduces the identifiability of that region. This is

the same effect as the general case when observation error variance is much larger than a parameter’s prior variance; i.e., the posterior is much more strongly determined by the prior than by the likelihood, resulting in limited Bayesian learning about quantities of interest.

It is common to plug in the MLEs of the GP covariance hyperparameters λ_η and β^η in (2) instead of including them in a full Bayesian analysis (Kennedy and O’Hagan, 2001; Santner et al., 2003; Qian et al., 2008; Paulo et al., 2012). In our proposed methodology, that is not merely a convenience, but rather is essential to avoid training an emulator using the target outcomes, which by their nature are extreme outliers (see Liu et al., 2009, on the dangers that arise here). We use values found by maximizing the log likelihood of the available simulation runs with respect to λ_η and β^η . We set the GP to have constant mean $c = 0$, which works well when (as here) the GP is not used for extrapolation (Bayarri et al., 2007). We set $\alpha_\eta = 2$, which assumes that the model output is infinitely differentiable.

We similarly model the discrepancy term $\delta(\cdot)$ as a mean-zero GP, with covariance function $C_\delta(\mathbf{x}, \mathbf{x}') = \lambda_\delta^{-1} \prod_{k=1}^p \exp(-\beta_k^\delta |x_k - x'_k|^{\alpha_\delta})$. This is included to capture systematic model bias. We use priors $\rho_k^\delta \sim \text{Beta}(1, 0.3)$, where $\rho_k^\delta = \exp(-\beta_k^\delta/4)$ for $k = 1, \dots, p$. Details of the prior for λ_δ are discussed below. As with the covariance function of $\eta(\cdot, \cdot)$, we set $\alpha_\delta = 2$.

Denote completed runs of the simulator $\boldsymbol{\eta} = (\eta(\mathbf{x}_1, \mathbf{t}_1), \dots, \eta(\mathbf{x}_n, \mathbf{t}_n))^T$, target outcomes $\mathbf{y} = (y(\mathbf{x}_{n+1}), \dots, y(\mathbf{x}_{n+m}))^T$, and $\mathcal{D} = (\boldsymbol{\eta}^T, \mathbf{y}^T)^T$. Then $\mathcal{D} | \boldsymbol{\theta}, \widehat{\lambda}_\eta, \widehat{\boldsymbol{\rho}}^\eta, \lambda_\delta, \boldsymbol{\rho}^\delta$ is multivariate normal with mean 0 and covariance $\mathbf{C}_\mathcal{D}$, a matrix with i, j entry equal to $C((\mathbf{x}_i, \mathbf{t}_i), (\mathbf{x}_j, \mathbf{t}_j)) + I(i, j > n) \cdot (C_{obs}(\mathbf{x}_i, \mathbf{x}_j) + C_\delta(\mathbf{x}_i, \mathbf{x}_j))$. $C_{obs}(\cdot, \cdot)$ serves as observation error variance, since we assume that in ω , the world in which the targets are observed, they

are subject to observation error. Whether this assumption is appropriate in a particular application will depend on the particulars of the phenomenon of interest. However, it is necessary to construct the model in such a way that the target outcomes are compossible with the model, and our assumption of Gaussian observation error ensures that this requirement is satisfied, even in cases where a model discrepancy term $\delta(\cdot)$ is not appropriate. Thus, $C_{obs}(\mathbf{x}_i, \mathbf{x}_j) = \sigma^2 \delta_{ij}^K$, where δ^K is the Kronecker delta and σ^2 is chosen to reflect the observation error. In our applications, we set $\sigma^2 = 0.05$ (with target outcomes standardized to have mean zero and standard deviation 1). $C_{obs}(\cdot, \cdot)$ also serves to add a nugget to the covariance matrix produced by $C_\delta(\cdot, \cdot)$. This improves the conditioning of the covariance matrix, and the addition of such a nugget can furthermore improve the fit of the GP discrepancy δ (Gramacy and Lee, 2012). Setting a uniform prior on the design variables $\boldsymbol{\theta}$, the joint posterior density under the model is

$$\pi(\boldsymbol{\theta}, \lambda_\delta, \boldsymbol{\rho}^\delta | \mathcal{D}, \widehat{\lambda}_\eta, \widehat{\boldsymbol{\rho}}^\eta) \propto \pi(\mathcal{D} | \boldsymbol{\theta}, \widehat{\lambda}_\eta, \widehat{\boldsymbol{\rho}}^\eta, \lambda_\delta, \boldsymbol{\rho}^\delta) \times \pi(\lambda_\delta) \times \pi(\boldsymbol{\rho}^\delta). \quad (3)$$

Markov chain Monte Carlo methods are used to explore the posterior distribution.

To successfully locate the optimal design region, one must either place an informative prior on the marginal precision λ_δ of the discrepancy $\delta(\cdot)$, or else specify λ_δ outright. Otherwise, the optimal region of the design variable space will suffer from poor identifiability, so that the posterior distribution will not be concentrated within the optimal region. This longstanding concern was raised in the discussion of Kennedy and O’Hagan (2001), as well as by Bayarri et al. (2007), Tuo and Wu (2015), and Plumlee (2017). How informative one’s prior on λ_δ will be depends upon how much one knows about the feasible design space prior to undertaking CTO.

Where the prior on λ_δ cannot be chosen to be *accurate* (due to insufficient prior knowledge) one should *overestimate* the precision. Otherwise, underestimation of λ_δ may lead to poor identifiability of the optimal design region by granting the model too much flexibility in systematically deviating from the targets. However, if λ_δ is too highly overestimated, MCMC may become trapped in a local mode, leading to convergence problems. In short, while the proposed methodology is forgiving of overestimation of λ_δ , the identifiability of the optimal design region(s) is best served by supplying as informative of a prior as possible.

When one lacks the prior knowledge necessary to select target outcomes near the feasible design space and an accurate prior for λ_δ , one option is a “preliminary round” of CTO to estimate the system’s Pareto front. As an example of preliminary CTO, consider again the univariate case, supposing now that we know only that the optimal output is approximately constant somewhere in the range $(0, 20)$. One can perform CTO with constant target outcome -1 but with a prior on λ_δ that deliberately exploits the identifiability problems of the Kennedy-O’Hagan framework in order to explore large regions of the parameter space – say, exponential with rate 0.1. The resulting posterior distribution will have greater density in the optimal region(s) than would a uniform sampling, but it will likely not center in the optimal region, instead covering a larger area of the design space. The posterior predictive distribution samples can be filtered to retain only their Pareto front, thereby estimating the true Pareto front in the vicinity of the target outcome. This estimate allows one to select a new set of target outcomes that is known to lie near the design space. Performing CTO with these new targets and an accurate, informative prior on λ_δ will result in a posterior distribution that concentrates on the optimal region, and the resulting posterior predictive

distribution will allow one to estimate optimal output with quantified uncertainty. The full CTO process, including preliminary Pareto front estimation, is given in Algorithm 1.

Algorithm 1: Full CTO procedure including preliminary estimation of Pareto front	
1.	Set target outcomes \mathbf{y} out of the feasible design space and a vague prior on λ_δ .
2.	Use MCMC to sample $\boldsymbol{\theta} \mathbf{y}$ and thereby the posterior predictive distribution.
3.	Filter the predictions to retain only their Pareto optimal values \mathcal{P} .
4.	Select new target outcomes \mathbf{y}^* using \mathcal{P} as an estimate of the model's Pareto front.
5.	Set a strong (or degenerate) prior on λ_δ with mean the distance from \mathcal{P} to \mathbf{y}^* .
6.	Use MCMC to draw from $\boldsymbol{\theta} \mathbf{y}^*$.

Figure 1 illustrates the benefits of preliminary CTO. Suppose that, prior to undertaking CTO, we know only that the model outputs are positive. Then $(0, 0)$ is a natural choice as a target outcome. However, firstly, the feasible design space is distant from $(0, 0)$, so that much of the design space is roughly as close to $(0, 0)$ as is the optimum, thus leading to poor identifiability of the optimal region. Secondly, the optimal region determined by the choice of $(0, 0)$ is arbitrary. The point closest to $(0, 0)$ is unique in the Pareto front solely in being nearest to the origin, and that choice of target outcome was itself driven merely by our ignorance of the feasible design space. By contrast, suppose now that preliminary CTO has supplied us a rough estimate of the Pareto front, empowering us to choose a different target outcome – for example, $(1.32, 0.065)$ targets a point of diminishing returns in allowing y_1 to increase further in exchange for a reduced y_2 . Such a new choice target outcome would answer both of the above problems. Note also that when an emulator is used, preliminary CTO can use the same model observations as the subsequent CTO to train the emulator. So preliminary CTO does not add to the budget of model runs, and is thus a computationally cheap supplement to CTO.

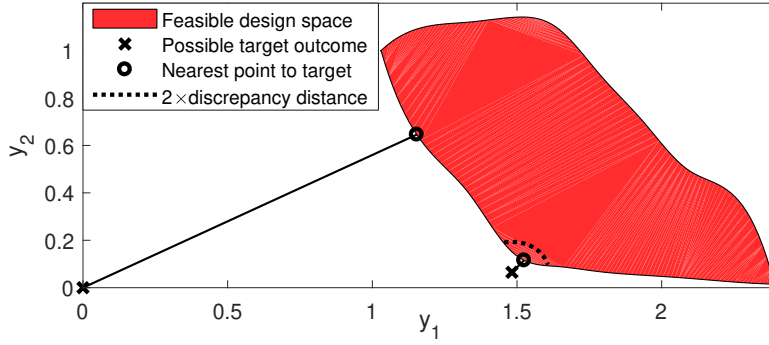


Figure 1: Two choices of target outcomes. The farthest point in the design space from $(0, 0)$ is only twice as far as the nearest point. By contrast, for $(1.32, 0.065)$, the dotted line shows the region of the design space within twice the distance to the nearest point.

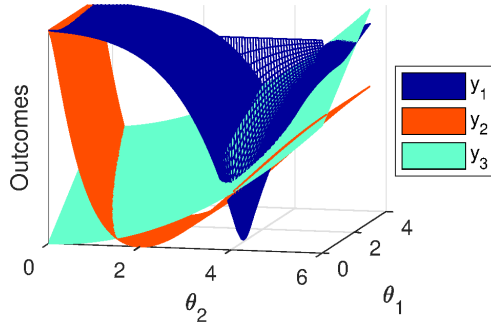


Figure 2: True outputs of the example model.

4 Simulated Example

To illustrate our proposed procedure, consider the following problem of minimizing a function with trivariate output. Let $(x, \boldsymbol{\theta})$ be the inputs, with scalar control input $x \in [1.95, 2.05]$ and design variables $\boldsymbol{\theta} = (\theta_1, \theta_2) \in [0, 3] \times [0, 6]$. We seek optimal settings for $\boldsymbol{\theta}$. Model outputs are $y_1 = (\theta_1 \exp(-(\theta_1 + |\theta_2 - \frac{\pi x}{2}|)) + 1)^{-1}$, $y_2 = (\theta_2^{x-1} \exp(-0.75\theta_2) + 1)^{-1}$, and $y_3 = 15 + 2\theta_1 + \theta_2^2/4$. We assume prior knowledge only that the outputs are positive. Figure 2 displays the (normalized) outputs as functions of θ_1 and θ_2 at $x = 2$. Assuming an easily evaluated model (so that an emulator is not needed), we have $\mathbf{z}(x) = \mathbf{f}(x, \boldsymbol{\theta}) + \delta(x) + \boldsymbol{\epsilon}$ for target outcome \mathbf{z} , where $\mathbf{f} = (y_1, y_2, y_3)^T$ is the output, $\delta(\cdot)$ is the discrepancy between

the optimal region and the target outcome, and $\epsilon \sim N(\mathbf{0}, 0.05I)$ is the tolerance.

We initially set the target outcomes to $(0, 0, 0)$, constant as a function of x . We estimated the Pareto front via preliminary CTO with $\lambda_\delta \sim \text{Exp}(1)$ to estimate its distance from the target outcome. Rescaling so that each output y is replaced with $\tilde{y} = (y - \mathbb{E}(y)) / \sqrt{\mathbb{V}(y)}$, the distance from the Pareto front to $(0, 0, 0)$ is 16 units. This is large compared to the size of the design space, at roughly four times its diameter. To improve identifiability of the optimal region, we updated the target outcome to lie along the line connecting the original target outcome to the nearest point of the estimated Pareto front, but now closer to the latter. We chose a distance of one unit away, as this is the standard deviation of each model output. We thereby approach the estimated Pareto front while remaining confident that the new target outcome $(0.71, 0.71, 17.92)$ outperforms the true Pareto front, since $F(\mathbf{x} - (0.71, 0.71, 17.92)^T) > 0.95$, where \mathbf{x} is the nearest point of the estimated Pareto front and F is the cdf of the tolerance $\epsilon \sim N(\mathbf{0}, 0.05I)$. For comparison, we also performed CTO directly, without preliminary CTO. To do so, we used our original target outcome $(0, 0, 0)$ with a $\text{Gamma}(10, 10)$ prior deliberately encouraging a large λ_δ . Figure 3 shows the resulting posteriors. The marginals in each case show substantial Bayesian learning compared to the prior (uniform) distribution of the design variables. CTO successfully maps the contours of the optimal region in each case, peaking near the true optimum. The benefits of preliminary CTO appear in the greater spread of the posterior distribution from direct CTO. The marginals are much more sharply peaked after preliminary CTO, with much lighter tails. This example illustrates that CTO can be used directly with little foreknowledge of a system’s Pareto front, but that greater identifiability of the optimal

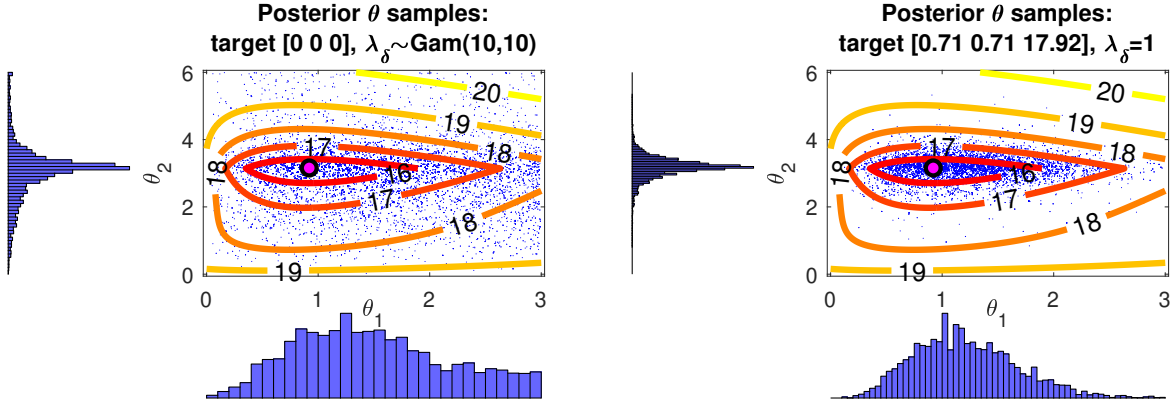


Figure 3: Posterior draws from CTO in the simulated example without and with the use of preliminary CTO. The contours show, for each point in the design space, the Euclidean distance of the model output at that point from the original target outcome (0,0,0), averaged across the control input range [1.95, 2.05]. The large dot shows the true optimum.

region can be achieved using preliminary CTO.

5 Application

In this section we use CTO to design a material for use in a wind turbine blade. The goal is to wed the typically separate tasks of material selection and material design, designing a composite to optimize performance in a blade. Our model uses ANSYS finite element analysis software (ANSYS, Inc., 2017). We assume the model accurately represents reality.

5.1 Wind turbine blade design

Two performance measures for blades are tip deflection and twist angle. A goal of engineering design is to keep these measures and material cost low. The blade is a composite of a given *matrix* and *filler*. In a composite, the matrix holds the filler together; for example in concrete, a filler of loose stones combines with a cement matrix. Given a matrix and

filler, the material properties (and thus blade performance and cost) depend on the thickness of the shear web in the blade and on the *volume fraction*, or ratio of filler to matrix. Temperature also affects the composite’s properties and hence performance. The model inputs are a triplet (h, v, k) , where h is the temperature of the turbine (in kelvin), v is the volume fraction, and k is the thickness (in mm). The model output is a triplet (d, r, c) , where d is tip deflection (in meters), r is twist (in radians), and c is cost per square meter (USD) of the material. The turbine is deemed to operate over temperatures 230K-330K.

5.2 Emulation of finite element model

The finite element simulator is too computationally expensive to be suitable for direct use in an MCMC routine. We employed a GP emulator in the manner of Williams et al. (2006). For this purpose, we drew 500 (trivariate) observations from the finite element simulator according to a Latin hypercube sampling design (McKay et al., 1979) based on plausible ranges for the three inputs as identified by subject matter experts: $[230\text{K}, 330\text{K}] \times [.2, .6] \times [10\text{mm}, 25\text{mm}]$. We took the computer output to follow a GP with mean 0 and product power exponential covariance function as given in (2). Since the model output is trivariate, we use two binary dummy variables a_1, a_2 to convert the model to univariate output with five inputs, in order to employ a univariate GP emulator. Thus for given values of h, v, k : setting $a_1 = a_2 = 0$ outputs the tip deflection d , setting $a_1 = 1$ and $a_2 = 0$ outputs the twist r , and settings $a_1 = 0$ and $a_2 = 1$ outputs the cost c .

The hyperparameters λ_η, β^η are estimated via maximum likelihood using only the finite element model output. We used `fmincon()` (MATLAB, 2017) to maximize (with $\mathcal{D} = \eta$)

over the joint (six-dimensional) support of β^η, λ_η . The result is that, following the form of Equation (2) with $p = 3$, $q = 2$, and $(x_1, x_2, x_3, t_1, t_2) = (a_1, a_2, h, v, k)$, we have $\hat{\lambda}_\eta = 0.0152$ and $\hat{\rho}^\eta = (0.9358, 0.6509, 0.6736, 0.4797, 0.9673)$, where $\rho_k^\eta = \exp(-\beta_k^\eta/4)$.

5.3 Design of the wind turbine blade system

All model inputs were rescaled to $[0,1]$. All model outputs were standardized so that each of the three responses has mean 0 and standard deviation 1. The full joint posterior density of the design variables and discrepancy function hyperparameters is given in Equation (3), using the MLEs given above. Initial target outcomes were set to $(0, 0, 0)$ on the original scale, constant as a function of temperature, on an evenly-spaced grid of temperature values over the range $[230\text{K}, 330\text{K}]$. We carried preliminary CTO with an $\text{Exp}(5)$ prior on λ_δ to estimate the Pareto front and update the target outcomes to lie close to the Pareto front. For this purpose, 2,000 realizations were drawn via Metropolis-Hastings-within-Gibbs MCMC (Metropolis et al., 1953; Hastings, 1970; Geman and Geman, 1984) in each of three chains (with random starts), of which the first 1,000 were discarded as burn-in. During the burn-in period, the covariances of the proposal distributions were periodically adjusted for optimal acceptance rates of around 23% for the multivariate θ and ρ^δ (Roberts et al., 1997) and 44% for the scalar λ_δ (Gelman et al., 2013, p. 296) using the sample covariance of the preceding draws. Convergence of the three chains was verified visually and by the Gelman-Rubin statistic (≈ 1.01 ; Gelman and Rubin, 1992).

As expected for preliminary CTO, the posterior distribution of θ was quite diffuse. We used the GP emulator to predict the model output for each realization of θ . Figure 4

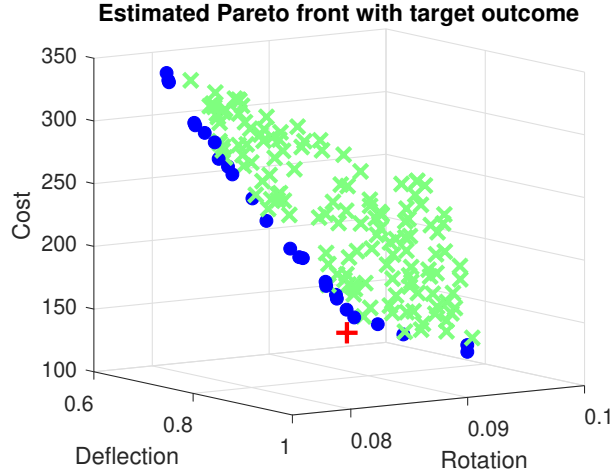


Figure 4: Each x is a dominated design drawn from the predictive distribution through preliminary CTO. The dots indicate the estimated Pareto front. The plus sign is the target selected as the performance objective in our proposed design approach.

displays the estimated Pareto front after filtering the posterior predictions to retain only non-dominated performance predictions. Though the design space is three-dimensional, the Pareto front appears to be a roughly coplanar curve describing a trade-off between cost and deflection/twist. A distinct point of maximum curvature appears in the Pareto front. This seems to be a point of diminishing returns in the trade-off between performance and cost, and thus we selected this point as the target for design. To do so, we set the point (deflection = 0.75m, twist = 0.09 rad, cost = \$130.34) as the target outcome, constant as a function of temperature. Based on the estimated Pareto front, the target outcome is approximately 0.2 units away on the standardized scale. Therefore, we set $\lambda_\delta = 1/0.2^2 = 25$.

In the subsequent CTO, we employed the same MCMC approach as in the preliminary round, except λ_δ was now fixed. The posterior distribution of θ appears in Figure 5 as contours of highest density regions. The contrast of the posterior distribution with the prior, which is uniform over the area shown in the figure, indicates that strong Bayesian learning

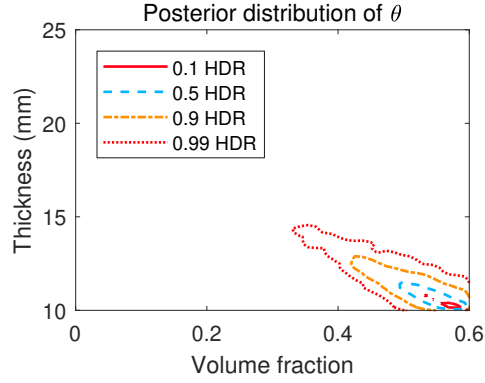


Figure 5: Contours of highest density regions of the posterior distribution from CTO in the wind turbine blade system. The prior is uniform over the area shown.

has occurred. The prior and posterior predictive distributions of the model outputs appear in Figure 6, where the prior predictive distributions are based on a uniform sampling of the model inputs. Each marginal posterior density peaks sharply near the target outcome. The

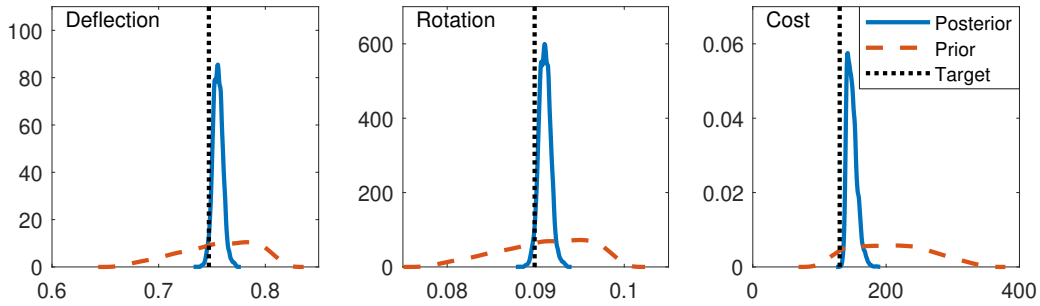


Figure 6: Approximate prior and posterior marginal predictive densities for each of the three outputs. Note that it is to be expected that the posteriors peak near the target (and not on it), since the target was intentionally chosen to lie outside the feasible design space.

mean output under the prior is $(0.76\text{m}, 0.09 \text{ rads}, \$207.90/\text{m}^2)$, and under the posterior it is $(0.76\text{m}, 0.09 \text{ rad}, \$149.47/\text{m}^2)$. Though the mean performance outcomes are approximately the same under the posterior and the prior, mean cost per square meter and the uncertainty of the outcomes are dramatically lower. If one prefers to prioritize gains in performance over cost, this can be accomplished by selecting target outcomes that reflect those priorities.

5.4 Pareto front estimation with quantified uncertainties

When multiple design outputs are to be minimized, any point in the Pareto front is optimal relative to some set of priorities. If those priorities have not been explicitly determined prior to the design process, then no particular outcome can be targeted. For example, in a system where performance is monotonically increasing in cost, depending on one's tolerance for high cost, any point in the design space might be optimal. In low-dimensional cases, CTO may be used to achieve a holistic picture of the Pareto front by optimizing to each target outcome on a grid. To do this, where the model output is d -dimensional, one may draw a grid over the range of $d - 1$ of the model outputs and perform CTO to minimize the remaining output at each point of the grid. The $d - 1$ outputs, at each grid point, are treated as known up to observation error (meaning that the discrepancy function $\delta(\cdot)$ is set to 0 in the dimension of these outputs). The resulting estimate of the Pareto front differs from the filtering method employed in preliminary CTO in that it allows for quantifying the uncertainty associated with the Pareto front.

Our proposed procedure is illustrated here using the wind turbine blade application. For simplicity, twist has been removed as a model output, leaving a system with 2-dimensional output of deflection and cost. The range of cost is known (via preliminary CTO) to be $[\$96, \$352]$. A 20-point grid was drawn over this range of costs. For each point c in the cost grid, we used the point $(0\text{m}, \$c)$ as the target outcome for calibration (constant with respect to temperature). For each such point, we then updated this initial target outcome to improve identifiability using the rough estimate of the Pareto front from preliminary CTO using target outcome $(0\text{m}, \$0)$. Note that only one round of preliminary CTO was

needed for this purpose, rather than a separate instance at each grid point.

The result is an estimate of the response surface with quantified uncertainty describing, for each point in the grid, the minimal achievable outcome for the output not included in the grid. The result of applying this strategy to the wind turbine blade application is shown in Figure 7. The lefthand plot shows that the posterior model predictions respected

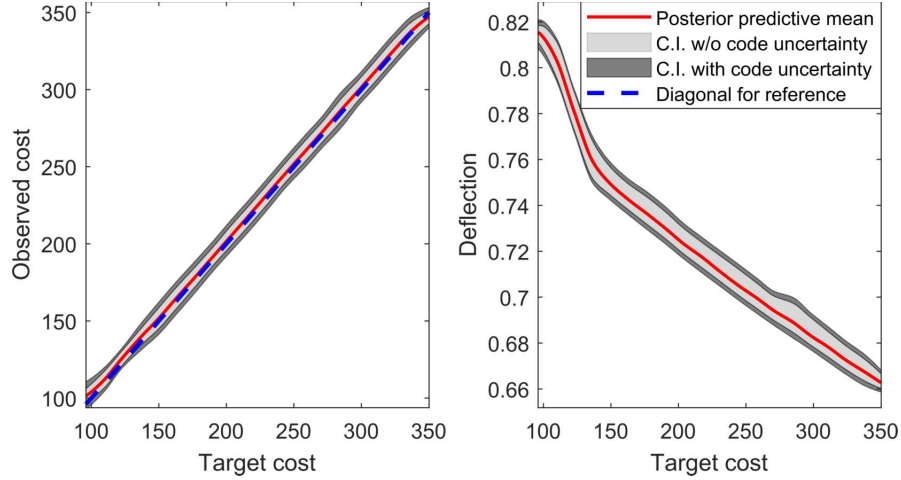


Figure 7: The lefthand plot shows the posterior predictive distribution of cost as a function of target cost, verifying that the calibration achieved the target costs up to small error. The righthand plot shows the Pareto front for the system with quantified uncertainty.

the target cost values used in the design process. The Pareto front for the system, along with associated uncertainty bands, appears in the righthand plot.

The use of CTO in the wind turbine design illustrates how preliminary CTO may be used, not merely to improve the identifiability of a pre-determined optimal region as in Section 4, but rather to identify a desirable region of the design space and select target outcomes that design to that region. In the wind turbine case, selecting $(0, 0, 0)$ as one's target determines the optimal region to be the high-cost region toward the upper-left of Figure 4, since (on the standardized scale of model outputs) that region happens to be

closest to the target. If one has substantive goals that drive one to select that target, then one is well-served by optimizing to that high-cost region. But if the target $(0, 0, 0)$ is chosen arbitrarily, then the resulting optimal region is itself determined arbitrarily. The estimate of the Pareto front provided by preliminary CTO allows us to identify regions of special interest, and to select target outcomes that lead to clearly defined designs, as illustrated in Figure 4.

The use of CTO in this case also demonstrates the value of obtaining a posterior distribution on the design variables, rather than just a point estimate. For example, Figure 5 shows not just that a reasonable point estimate of the optimal θ is at $(.58, 10.2\text{mm})$, but also that if the volume fraction is lowered to 0.4 it is important to simultaneously raise the thickness to 14mm. More generally, CTO delivers an indication of the range of θ values that achieve results near the target, which is potentially useful when one’s goal is to set tolerances (rather than a specific value) for θ . Finally, the use of CTO in the wind turbine case illustrates how the method can deliver “Pareto bands”, providing not merely an estimate of the Pareto front (as in preliminary CTO) but also uncertainty associated with that estimate. Such an estimate can be of use to decision-makers when deciding on performance goals subject to budgetary constraints.

6 Conclusion

We have described how the computer model calibration framework of Kennedy and O’Hagan (2001) can be adapted for engineering design. Calibration to target outcomes undertakes design by “calibrating” a model not to field observations, but rather to artificial data repre-

senting performance and cost targets. The procedure optionally includes a computationally cheap preliminary step that provides a rough estimate of the Pareto front, which may be used to select target outcomes that promote strong Bayesian learning. The resulting posterior predictive distribution approximates the target outcomes, so that the posterior distribution of θ constitutes a distribution on optimal design settings. Repeated applications of this methodology could allow one to construct a thorough estimate of the Pareto front of the system with quantified uncertainties by selecting target outcomes that explore different portions of the Pareto front. Unlike other methods of Bayesian optimization (a review of which is provided by Shahriari et al. 2016), CTO does not require the ability to evaluate model output adaptively. Instead, it can rely on a batch of observations gathered prior to (and independently of) the design process. We described the implementation of this approach in an MCMC routine along with considerations to accommodate computational instability. The use of this methodology is illustrated in the case of material design for a wind turbine blade. By expropriating established tools of model calibration, CTO offers a method of optimization which is sensitive to, and quantifies, all sources of uncertainty.

The methodology as described here treats the computer model as universally valid over the domain of the design variables. Future work in this area will include the use of a second discrepancy term capturing model bias. Other possible extensions of our proposed methodology include its application to so-called “state-aware calibration” (Atamturktur and Brown, 2015; Stevens et al., 2018; Brown and Atamturktur, 2018), which would allow the optimal region of the design variables to vary as a function of the control inputs.

SUPPLEMENTARY MATERIAL

Matlab code for CTO: This includes code to perform CTO on the example model of Section 4, reproducing Figure 3. (Zipped Matlab .m scripts and .mat file)

FE model description: This describes the background and FE implementation of the CX-100 wind turbine blade analyzed in this paper. (.pdf file)

FE implementation: This includes Matlab and ANSYS files to model the blade along with airfoil profiles and macro files used during blade geometry generation. (.zip file)

References

Adams, R. M. (1974). Theories of Actuality. *Noûs* 8(3), 211.

ANSYS, Inc. (2017). Ansys® academic research mechanical, release 18.1.

Atamturktur, S. and D. A. Brown (2015). State-aware calibration for inferring systematic bias in computer models of complex systems. *NAFEMS World Congress Proceedings, June 21-24*.

Bastos, L. S. and A. O’Hagan (2009). Diagnostics for Gaussian process emulators. *Technometrics* 51(4), 425–438.

Bayarri, M. J., J. O. Berger, J. Cafeo, G. Garcia-Donato, F. Liu, J. Palomo, R. J. Parthasarathy, R. Paulo, J. Sacks, and D. Walsh (2007). Computer model validation with functional output. *The Annals of Statistics* 35, 1874–1906.

Bayarri, M. J., J. O. Berger, R. Paulo, J. Sacks, J. A. Cafeo, J. Cavendish, C.-H. Lin, and

- J. Tu (2007). A framework for validation of computer models. *Technometrics* 49(2), 138–154.
- Brown, D. A. and S. Atamturktur (2018). Nonparametric functional calibration of computer models. *Statistica Sinica* 28, 721–742.
- Brynjarsdóttir, J. and A. O’Hagan (2014). Learning about physical parameters: The importance of model discrepancy. *Inverse Problems* 30(11).
- Chevalier, C., J. Bect, D. Ginsbourger, E. Vazquez, V. Picheny, and Y. Richet (2014). Fast Parallel Kriging-Based Stepwise Uncertainty Reduction With Application to the Identification of an Excursion Set. *Technometrics* 56(4).
- Deb, K. and H. Gupta (2006, dec). Introducing robustness in multi-objective optimization. *Evolutionary Computation* 14(4), 463–494.
- Gelfand, A. E. and A. F. M. Smith (1990, jun). Sampling-based approaches to calculating marginal densities. *Journal of the American Statistical Association* 85(410), 398–409.
- Gelman, A., J. B. Carlin, H. S. Stern, D. B. Dunson, A. Vehtari, and D. B. Rubin (2013). *Bayesian data analysis* (3rd ed.). London: CRC Press.
- Gelman, A. and D. B. Rubin (1992). Inference from Iterative Simulation Using Multiple Sequences. *Statistical Science* 7(4), 457–472.
- Geman, S. and D. Geman (1984). Stochastic relaxation, Gibbs distributions, and the Bayesian restoration of images. *IEEE Transactions on Pattern Analysis and Machine Intelligence* 6(6), 721–741.

- Gramacy, R. B. and H. K. H. Lee (2008). Bayesian treed Gaussian process models with an application to computer modeling. *Journal of the American Statistical Association* 103(483), 1119–1130.
- Gramacy, R. B. and H. K. H. Lee (2012). Cases for the nugget in modeling computer experiments. *Statistics and Computing* 22(3), 713–722.
- Hastings, W. (1970). Monte Carlo sampling methods using Markov chains and their applications. *Biometrika* 57(1), 97–109.
- Hemez, F. and S. Atamturktur (2011). The dangers of sparse sampling for the quantification of margin and uncertainty. *Reliability Engineering & System Safety* 96(9), 1220–1231.
- Higdon, D., M. Kennedy, J. C. Cavendish, J. A. Cafo, and R. D. Ryne (2004). Combining field data and computer simulations for calibration and prediction. *SIAM Journal on Scientific Computing* 26(2), 448–466.
- Jin, Y. and J. Branke (2005). Evolutionary optimization in uncertain environments - A survey. *IEEE Transactions on Evolutionary Computation* 9(3), 303–317.
- Jones, D. R., M. Schonlau, and W. J. Welch (1998). Efficient Global Optimization of Expensive Black-Box Functions. Technical report.
- Kennedy, M. C., C. W. Anderson, S. Conti, and A. O’Hagan (2006). Case studies in Gaussian process modelling of computer codes. *Reliability Engineering & System Safety* 91(10-11), 1301–1309.

- Kennedy, M. C. and A. O’Hagan (2001). Bayesian calibration of computer models. *Journal of the Royal Statistical Society: Series B* 63(3), 425–464.
- Lewis, D. K. (1986). *On the plurality of worlds*. Blackwell.
- Liu, F., M. J. Bayarri, and J. O. Berger (2009). Modularization in Bayesian analysis, with emphasis on analysis of computer models. *Bayesian Analysis* 4(1), 119–150.
- Loeppky, J. L., D. Bingham, and W. J. Welch (2006). *Computer model calibration or tuning in practice*. University of British Columbia: Department of Statistics.
- MATLAB (2017). *Version 9.2.0 (R2017a)*. Natick, Massachusetts: The MathWorks, Inc.
- McKay, M. D., R. J. Beckman, and W. J. Conover (1979). Comparison of three methods for selecting values of input variables in the analysis of output from a computer code. *Technometrics* 21(2), 239–245.
- Metropolis, N., A. W. Rosenbluth, M. N. Rosenbluth, A. H. Teller, and E. Teller (1953). Equation of state calculations by fast computing machines. *The Journal of Chemical Physics* 21(6), 1087–1092.
- Miettinen, K. (2008). *Introduction to Multiobjective Optimization: Noninteractive Approaches*, pp. 1–26. Berlin, Heidelberg: Springer Berlin Heidelberg.
- O’Hagan, A. (1978). Curve fitting and optimal design for prediction. *Journal of the Royal Statistical Society: Series B* 40(1), 1–42.
- Olalotiti-Lawal, F. and A. Datta-Gupta (2015, sep). A Multi-Objective Markov Chain

- Monte Carlo Approach for History Matching and Uncertainty Quantification. In *SPE Annual Technical Conference and Exhibition*. Society of Petroleum Engineers.
- Paulo, R., G. García-Donato, and J. Palomo (2012). Calibration of computer models with multivariate output. *Computational Statistics and Data Analysis* 56, 3959–3974.
- Picheny, V. (2015). Multiobjective optimization using Gaussian process emulators via stepwise uncertainty reduction. *Statistics and Computing* 25(6), 1265–1280.
- Picheny, V., M. Binois, and A. Habbal (2019, jan). A Bayesian optimization approach to find Nash equilibria. *Journal of Global Optimization* 73(1), 171–192.
- Plumlee, M. (2017). Bayesian calibration of inexact computer models. *Journal of the American Statistical Association* 112(519), 1274–1285.
- Pratola, M. and O. Chkrebtii (2018). Bayesian calibration of multistate stochastic simulators. *Statistica Sinica* 28, 693–719.
- Qian, P. Z. G., H. Wu, and C. F. J. Wu (2008). Gaussian process models for computer experiments with qualitative and quantitative factors. *Technometrics* 50(3), 383–396.
- Roberts, G., A. Gelman, and W. Gilks (1997). Weak convergence and optimal scaling of random walk Metropolis algorithms. *The Annals of Applied Probability* 7(1), 120.
- Sacks, J., W. J. Welch, T. J. Mitchell, and H. P. Wynn (1989). Design and analysis of computer experiments. *Statistical Science* 4(4), 409–423.
- Santner, T. J., B. J. Williams, and W. I. Notz (2003). *The design and analysis of computer experiments*. New York: Springer.

- Shahriari, B., K. Swersky, Z. Wang, R. P. Adams, and N. de Freitas (2016). Taking the human out of the loop: A review of Bayesian optimization. *Proceedings of the IEEE* 104(1), 148–175.
- Stevens, G. N., S. Atamturktur, D. A. Brown, B. J. Williams, and C. Unal (2018). Statistical inference of empirical constituents in partitioned analysis from integral-effect experiments. *Engineering Computations* 35(2), 672–691.
- Tuo, R. and C. F. J. Wu (2015). Efficient calibration for imperfect computer models. *Annals of Statistics* 43(6).
- Tuo, R. and C. F. J. Wu (2016). A theoretical framework for calibration in computer models: Parametrization, estimation and convergence properties. *SIAM/ASA Journal on Uncertainty Quantification* 4(1), 767–795.
- Van Buren, K. L., S. Atamturktur, and F. M. Hemez (2014). Model selection through robustness and fidelity criteria: Modeling the dynamics of the CX-100 wind turbine blade. *Mechanical Systems and Signal Processing* 43(1-2), 246–259.
- Van Buren, K. L., M. G. Mollineaux, F. M. Hemez, and S. Atamturktur (2013). Simulating the dynamics of wind turbine blades: Part II, model validation and uncertainty quantification. *Wind Energy* 16(5), 741–758.
- Williams, B., D. Higdon, J. Gattiker, L. Moore, M. McKay, and S. Keller-McNulty (2006). Combining experimental data and computer simulations, with an application to flyer plate experiments. *Bayesian Analysis* 1(4), 765–792.

Young, M. (1994). *The Guinness book of records, 1995*. Facts on File.

Zhou, Q., P. Z. G. Qian, and S. Zhou (2011). A simple approach to emulation for computer models with qualitative and quantitative factors. *Technometrics* 53(3), 266–273.